

Siderophile Element Constraints on the Formation of Metal in the Metal-rich Chondrites Bencubbin, Weatherford, and Gujba

ANDREW J. CAMPBELL*¹, MUNIR HUMAYUN¹, AND MICHAEL K.
WEISBERG²

¹Department of the Geophysical Sciences, The University of Chicago, Chicago, Illinois
60637, USA

²Department of Physical Sciences, Kingsborough College of the City College of New
York, Brooklyn, New York 11235, USA

*email: acampbel@midway.uchicago.edu

ph: (773) 834-1523, fax: (773) 702-9505

Submitted to *Geochim. Cosmochim. Acta*, 19 April 2001

Revised: 2 August 2001

Abstract—Laser ablation ICP mass spectrometry was used to measure abundances of P, Cr, Fe, Co, Ni, Cu, Ga, Ge, As, Mo, Ru, Rh, Pd, Sn, Sb, W, Re, Os, Ir, Pt, and Au in metal grains in the Bencubbin-like (CB) chondrites Bencubbin, Weatherford, and Gujba to determine the origin of large metal aggregates in bencubbinites. A strong volatility-controlled signature is observed among the metal grains. The refractory siderophiles Ru, Rh, Re, Os, Ir, and Pt are unfractionated from one another, and are present in approximately chondritic relative abundances. The less refractory elements Fe, Co, Ni, Pd, and Au are fractionated from the refractory siderophiles, with a chondritic Ni/Co ratio and a higher than chondritic Pd/Fe ratio. The moderately volatile siderophile elements Ga, Ge, As, Sn, and Sb are depleted in the metal, relative to chondritic abundances, by up to three orders of magnitude. The trace siderophile element data are inconsistent with the following proposed origins of Bencubbin-Weatherford-Gujba metal: 1) condensation from the canonical solar nebula; 2) oxidation of an initially chondritic metal composition; and 3) equilibration with a S-rich partial melt. A condensation model for metal-enriched ($\times 10^7$ CI) gas is developed. Formation by condensation or evaporation in such a high density, metal-enriched gas is consistent with the trace element measurements. The proposed model for generating such a gas is protoplanetary impact involving a metal-rich body.

1. INTRODUCTION

The role of impacts in the formation of chondrites, their chondrules and distinctive chemical fractionations, and in the early thermal and chemical evolution of planetesimals may be comparable in importance to nebular processes. Although most proposals for the formation of chondrules have a nebular setting (Boss, 1996), Zook (1981) and Wänke et al. (1981) proposed a model involving collisions of partially molten planetesimals heated by ^{26}Al decay, which also accounted for the large-scale volatile element depletions observed in chondrites. Lugmair and Galer (1992) proposed a similar model to understand the early formation of volatile-poor achondrites, particularly angrites. Chen et al. (1998) invoked such models to explain the Re/Os fractionations observed in ordinary chondrite metal. Wasson and Kallemeyn (1990) and Kallemeyn et al. (2001) proposed, on the basis of petrographic studies and neutron activation analyses of sample separates, that the CH chondrite Allan Hills (ALH) 85085 and the bencubbinite (CB chondrite) Gujba formed by condensation from impact-derived vapor clouds.

Bencubbinites are primitive, metal-rich breccias that are closely related to the CR and CH chondrites (Weisberg et al., 1998; 2001). In addition to the Kallemeyn et al. (2001) model, proposed origins of metal in the CB, CH, and CR carbonaceous chondrite classes have included condensation from the solar nebula (Grossman and Olsen, 1974; Newsom and Drake, 1979; Meibom et al., 1999; 2000; Weisberg et al., 1990; 2001), reduction of FeO from coexisting silicates (Lee et al., 1992), and solidification from impact-induced melt (Kallemeyn et al., 1978). These arguments were based primarily on electron microprobe measurements of Ni, Co, Cr, and P in chondritic metals, which cover a limited range in terms of their condensation temperatures and redox properties. In the present study laser ablation inductively coupled plasma mass spectrometry (LA-ICP-MS) was used to determine the abundances of 22 siderophile and chalcophile elements, including P, Cr, Fe, Co, Ni, all of the refractory siderophiles and most of the volatile siderophiles, in bencubbinite metal. The chemical consequences of an equilibrium

condensation origin of metal from a vapor cloud substantially enriched in siderophiles relative to nebular models, such as might be produced by impact-induced vaporization of metal-rich chondrites, are developed and explored here. The LA-ICP-MS results are compared with the siderophile element patterns from models of each of the proposed origins of this metal.

Bencubbinite metal occurs as three types: as large sulfide-bearing aggregates, as homogeneous sulfide-free grains, and as sulfide-free grains that are zoned in Ni and other siderophiles (Weisberg et al., 2000). The metal has not decomposed to kamacite + taenite, even in Ni-rich regions; this apparent lack of thermal metamorphism has contributed to the description of these meteorites as 'primitive' (Newsom and Drake, 1979; Weisberg et al., 1990; 2001). Similar zoned metal grains have been described in CH meteorites by Meibom et al. (1999), who interpreted these textures in terms of condensation of the metal grains from the solar nebula (Meibom et al., 1999; 2000). Silicates occur primarily as barred olivine or cryptocrystalline chondrules showing no sign of secondary alteration (Newsom and Drake, 1979; Weisberg et al., 1990; 2001; Krot et al., 2001). A metal/silicate intergrowth, comprising <1% of each bencubbinite, binds the metal and silicate clasts together, and has been interpreted by all investigators as a shock melt (Ramdohr, 1973; Kallemeyn et al., 1978; Newsom and Drake, 1979; Weisberg et al., 1990; Meibom et al., 2000).

Weisberg et al. (2001) divided the CB chondrites into two subgroups, with Bencubbin and Weatherford in CB_a and QUE 94411 and HH 237 in CB_b. Weisberg et al. (2001) did not study Gujba, but petrological and geochemical study of Gujba links it to the CB_a group (Rubin et al., 2001). The bulk Ni-normalized siderophile and Mg-normalized lithophile contents of CB_a chondrites are close to those of CB_b chondrites (Weisberg et al., 2001; Kallemeyn et al., 2001), and the high metal/silicate ratios in these meteorites are also similar. They also share similar oxygen isotope compositions, plotting near the CR line, and all have high $\delta^{15}\text{N}$ values of ~200 to 1000 ‰ (Prombo and Clayton, 1978; Sugiura et

al., 2000; Weisberg et al., 2001). Grain sizes of metal and silicate in the CB_a subgroup are generally larger than those in the CB_b subgroup (Weisberg et al., 2001). CB_b chondrites do contain sulfide-bearing metal aggregates, but they are much less common than in the CB_a chondrites. The CB_b subgroup contains both zoned metal and CAIs, but the CB_a group contains neither (Weisberg et al., 2001).

Zoned metal in the bencubbinites Queen Alexandra Range (QUE) 94411 and Hammadah al Hamra (HH) 237 has been analyzed for platinum group element (PGE) distributions, and the results supported a nebular condensation origin for the siderophile element enrichments in the cores of these grains (Campbell et al., 2000; 2001a). The unzoned metal in bencubbinites exhibits a positive Ni-Co correlation that has also been interpreted to result from a nebular condensation process (Newsom and Drake, 1979; Weisberg et al., 1990; 1999; 2001). Here, we report siderophile element measurements for Bencubbin, Weatherford, and Gujba metal clasts, which permit a comparison between the origins of zoned and unzoned metal in CB chondrites. Preliminary results from this study were presented by Campbell and Humayun (2000) and Campbell et al. (2001b).

2. EXPERIMENTAL

Sections of Bencubbin, Weatherford, and Gujba were examined optically and by SEM (JEOL 5800-LV, University of Chicago) to select target areas for LA-ICP-MS analyses. A CETAC LSX-200 laser ablation peripheral was used with a magnetic sector inductively coupled plasma mass spectrometer (LA-ICP-MS), the Finnigan Element™ (Campbell and Humayun, 1999ab; Campbell et al., 2001a). Each point analysis on the sample produced a pit 25-150 μm in diameter and 15-35 μm deep. On large (mm-sized) aggregates, the laser was rastered over the sample during data collection. The isotopes ³¹P, ³⁴S, ⁵³Cr, ⁵⁷Fe, ⁵⁹Co, ⁶⁰Ni, ⁶³Cu, ⁶⁹Ga, ⁷⁴Ge, ⁷⁵As, ⁹⁵Mo, ¹⁰¹Ru, ¹⁰³Rh, ¹⁰⁵Pd, ¹¹⁸Sn, ¹²¹Sb, ¹⁸²W, ¹⁸⁵Re, ¹⁹²Os, ¹⁹³Ir, ¹⁹⁵Pt, and ¹⁹⁷Au were monitored during some or all of the measurements. During single point analyses, the signal rapidly increased to a maximum

and then decayed toward background levels as the transient pulse of ablated material passed through the instrument; when the laser was being rastered over a larger area, the signal remained more steady. In both methods the ICP-MS was swept repeatedly across the masses of interest, with sampling times of 20-30 ms per peak on each sweep. Each sweep duration spent 50-60% on peak, and the intensity data were integrated over a ~20 s period.

Instrumental sensitivity factors for each isotope relative to ^{57}Fe were determined by measuring signal intensity from metal standards which have known concentrations of the elements of interest (Campbell and Humayun, 1999b; Campbell et al., 2001a); these standards included the iron meteorites Hoba IVB (Co, Ni, PGEs, Re, Au), Filomena IIA (Ga, Ge, As, W), and the NIST SRMs 1158 (S, Cr, Cu, Mo) and 1263a (P, S, Cu, As, Mo, Sn, Sb, W, Au). The corrected intensities were converted to elemental abundances by normalization to $[\text{Fe}] + [\text{Co}] + [\text{Ni}] = 100 \text{ wt\%}$. Precision of the LA-ICP-MS measurements, as calculated from counting statistics or from replicate measurements, varied with spot size and was typically 5-20% (2σ). The 2σ errors are shown with the data in the figures. A comparison between the compositions of the standards, as determined from 5 replicate LA-ICP-MS point analyses, and the values reported in the literature is given in Table 1.

3. RESULTS

The metal observed in these meteorites occurs primarily in two textural-compositional forms: large, sulfide-bearing metal aggregates approximately 1-10 mm in size, and homogeneous grains 0.1-1 mm in size (Weisberg et al., 2000; Rubin et al., 2001) (Figure 1a). The aggregates consist of sulfide-free and sulfide-bearing grains, that are sintered together, with sulfide blebs frequently occurring at the grain margins (Figure 1). Sulfide within grains is usually rounded, 1-10 μm in diameter; sulfide at the internal grain margins of the aggregates often delineates triple junction forms in the metal aggregates. In the Bencubbin section studied, the metal fraction was ~60 vol%. The Gujba mount

contained two metal aggregates that had been separated from the meteorite, and one of the Gujba aggregates had an additional homogenous grain of different composition attached to it. The two Weatherford sections contained a total of 4 metal clasts, one of which is presented in Figure 1b. Nickel concentrations at the cores and rims of metal grains were measured by EDX; none of the metal was found to be zoned, in contrast to that found in the bencubbinites QUE 94411 and HH 237 (Weisberg et al., 2000).

LA-ICP-MS data for metal in Bencubbin, Weatherford, and Gujba are listed in Table 2. Each entry represents a single aggregate or homogeneous grain; when multiple measurements were made on the same metal sample, the results were averaged in Table 2. In order to enhance the precision and sensitivity of the LA-ICP-MS measurement for a particular set of elements, other elements (e.g., As, Sn, and Sb in Bencubbin) were sometimes excluded from the analysis. In addition to the elements listed in Table 2, an attempt was made to measure Ag in clast A of Bencubbin. After removal of ubiquitous surface Ag contaminant by pre-ablating the surface with the laser, an upper limit of 0.5 ppb was set for Ag in this clast, with a Pd/Ag ratio ≥ 6000 .

Figure 2 shows the abundances of the siderophile elements in individual clasts from Bencubbin, Weatherford, and Gujba, plotted in order of increasing volatility (Campbell et al., 2001a; Wai and Wasson, 1977). These data, in agreement with previous measurements on the bulk meteorites (Kallemeyn et al., 1978), show that the refractory siderophiles are, on average, enriched in this metal by a few tens of percent relative to Fe, and the volatile elements are depleted by orders of magnitude.

The refractory PGEs (Ru, Rh, Os, Ir, and Pt), Mo, and Re were found to behave similarly to one another in all three meteorites. This is demonstrated in Figure 3, in which several siderophile element abundances from all three meteorites are plotted. The elements Mo, Ru, Rh, Os, Pt, and Re are all essentially unfractionated from Ir, and are present in nearly chondritic relative abundances, even as Ir varies by a factor of ~ 3 . The scatter in Mo/Ir and W/Ir is greater than that for the other refractory siderophile ratios, and well

beyond analytical uncertainties. The elements Pd and Au are correlated with Ir, but there is significant Pd/Ir and Au/Ir fractionation evident in Figure 3. Both of these elements are depleted relative to Ir at high Ir concentrations in the Bencubbin-Weatherford-Gujba metal.

The Co/Ni ratio is also nearly chondritic in all measurements; this is in agreement with previous studies (Newsom and Drake, 1979; Weisberg et al., 1990). Other minor elements, such as P, S, and Cr, do not correlate strongly with Ni. Newsom and Drake (1979) discussed the genetic implications of P-Ni and Cr-Ni trends in Bencubbin, but the data in that study had a large degree of scatter. Further, Ni does not correlate with many of the moderately volatile trace elements (Ga, Ge, As, Sn, Sb, Au), nor with W.

There are, however, strong correlations between Ni and other refractory siderophiles such as the PGEs, Mo, and Re. Since the refractory PGEs, plus Re, vary in unfractionated proportions in Bencubbin-Weatherford-Gujba metal (Figure 3), we adopt Ir as representative of these elements, and it is to be understood that the other refractory PGEs plot similarly to Ir. The Ir/Fe ratios for each metal sample are plotted against Ni/Fe in Figure 4. Metal clasts in Bencubbin extend along a linear trend from almost chondritic abundances, where Ni ~5.5 wt% and Ir ~2.4 ppm, to higher Ni and Ir contents reaching 7.1 wt% Ni and 4.5 ppm Ir. The Gujba and Weatherford data plot close to those of Bencubbin, and in most of this paper we consider the metal from all three meteorites to have had a common origin. Two of the four Weatherford data are outliers from the trend defined by the other data, but because of the limited number of data available, we make little attempt to interpret these outliers. A similar plot of Pd/Fe vs. Ni/Fe is also shown in Figure 4. In all three meteorites, Pd is positively correlated with Ni, and again the Pd-Ni trend passes near the chondritic abundances.

4. DISCUSSION

4.1 Chemical Fractionations in Bencubbin, Weatherford, and Gujba Metal

There have been several proposals to explain the origin of the host metal in Bencubbin, Weatherford, and Gujba (Kallemeyn et al., 1978; 2001; Newsom and Drake, 1979; Weisberg et al., 1990; 2001; Rubin et al., 2001), and the trace siderophile element data provide important tests of each of these models.

Kallemeyn et al. (1978) interpreted their neutron activation analysis results from Bencubbin and Weatherford in terms of an impact-generated magma, consisting of molten metal and silicate. However, the bulk compositional studies of Kallemeyn et al. (1978) did not recognize the compositional variability among the host metal clasts. Newsom and Drake (1979) documented trends among major and minor element compositions within the Bencubbin host metal clasts, and they rejected the impact melt model of Kallemeyn et al. (1978), partly because the bulk metal abundances of Ir and Re reported by Kallemeyn et al. (1978) did not show the strong fractionation away from solar ratios that is observed in the magmatic iron meteorite groups. Fractional crystallization would produce very strong elemental fractionations, by orders of magnitude, that are not observed (Table 1 and Figure 4). Alternatively, one might consider an equilibrium partial melting model, in which each metal clast equilibrated with a melt under different conditions of temperature or bulk (solid + liquid) composition. At low degrees of partial melting and high S contents of the melt, Ni becomes a compatible element, and models can be constructed in which a positive correlation exists between Ni and Ir or Pd (Jones and Malvin, 1990). However, under these conditions we find that other important constraints (e.g., the chondritic Co/Ni ratio) are violated, and therefore a partial melt origin may also be rejected as the cause of the trace element signatures of the metal in Bencubbin, Gujba, and Weatherford.

Various chondritic metals have been proposed to have been formed by redox processes occurring on the parent body (Lee et al., 1992; Zanda et al., 1994). The suggestion of Weisberg et al. (1990; 1999) that the solar Co/Ni ratio in Bencubbin metal

could also have been maintained by subsolidus oxidation and/or sulfidation can also be examined with the PGE data. In this model, the metal would have to have been metamorphosed at relatively high temperatures (>1000 K), with relatively rapid cooling to avoid extensive kamacite exsolution. Highly siderophile elements will not be fractionated from one another during this sort of redox processing; the Pd/Ir and Au/Ir fractionations presented in Figure 4 are therefore inconsistent with this mechanism. Similarly, loss of Fe during oxidation of the metal should produce trends on PGE/Fe vs. Ni/Fe plots that intercept (extrapolate to) the origin and are linear, reflecting a constant PGE/Ni ratio. The Pd/Fe vs. Ni/Fe plot in Figure 4 may be consistent with such a process, but the other PGEs, represented by Ir in Figure 4, show significant PGE/Ni fractionations at high Ni, and the redox trend drawn in this figure does not match the data.

The data in Figure 3 point strongly to volatility as the chemical property that controlled the fractionation of siderophiles. The refractory elements Mo, Ru, Rh, Re, Os, Ir, and Pt behave identically in this data set, while the less refractory elements Pd and Au are fractionated from the others at high Ir contents. The metal clasts in Bencubbin, Weatherford, and Gujba must have been produced by a volatility-controlled process, and not one dominated by oxidation/sulfidation or magmatic crystallization. This is equally evident in Figure 2, in which volatility plays an obvious role in controlling the chemical abundances.

An exception to the volatility control over elemental abundances may exist in the case of Mo and W, which both exhibit large scatter in Figure 3 relative to most other siderophiles. Since Mo and W differ from Ir in their sensitivity to oxidation, but are similar to Ir in being much more refractory than Fe, we might consider Mo/Ir or W/Ir to be indicators of redox processes. These two ratios are plotted against one another in Figure 5; the positive correlation in this figure implies that variations in oxidation state were responsible for the scatter around the trend in the Mo/Ir and W/Ir plots. Tungsten shows greater sensitivity to oxidation than Mo, as indicated by the large W/Ir range in Figure 5,

and this sensitivity disrupted the W/Ir ratio to a greater extent than the Mo/Ir ratio (Figure 3). Therefore, although the gross features of the trace element data in Bencubbin, Weatherford, and Gujba metal preclude an origin of the metal by oxidative loss of Fe, there is a detectable imprint of redox processing in the Mo and W abundances. Any proposed origin for these meteorites must not only involve a predominantly volatility-controlled process to explain the relations between highly siderophile elements, but must also allow for varying oxidation state to perturb the Mo and W abundances, as discussed further in a later section.

4.2 Condensation of Metal Alloy from the Solar Nebula

Newsom and Drake (1979) proposed that the compositions of Bencubbin metal were largely established during condensation from the solar nebula. This conclusion was based largely on the Co/Ni ratio, which remains nearly identical to that of CI chondrites as the Ni content varies among metal clasts; this was predicted by Grossman and Olsen (1974) to occur during condensation of metal from the solar nebula. Newsom and Drake (1979) offered the P-Ni correlation as further support for condensation, although the scatter in these data was large. They also noted that the low Ga and Ge contents reported by Kallemeyn et al. (1978) supported a condensation origin for Bencubbin metal. Weisberg et al. (1990) tentatively concluded that the host metal in Bencubbin may have formed by condensation, although they also considered alternatives such as impact melting, with “nonmagmatic” processing of metal similar to that observed in IAB iron meteorites, and late-stage oxidation and/or sulfidation, that can maintain an approximately solar Co/Ni ratio.

The proposed condensation origin for metal in Bencubbin (and, by analogy, in Weatherford and Gujba) is re-examined with the present trace element data. As discussed by Campbell et al. (2001a), the platinum group elements are an important set of elements with which to identify volatility-related processes in meteoritic metals because they are all

highly siderophile and they encompass a range of volatilities, from Os, which is one of the most refractory elements, to Pd, which has a volatility similar to that of Fe under nebular conditions. As shown in Figure 3, the refractory PGEs behave similarly to one another in Bencubbin, Weatherford, and Gujba metal, and Ir was shown as representative of the group in Figure 4. These elements are enriched in the metal, and are positively correlated with Ni. For comparison, the Ir-Ni trajectory expected for condensation of metal alloy from the solar nebula (Campbell et al., 2001a) is shown. The measured Ir-Ni trend for Bencubbin, Weatherford, and Gujba metal is significantly different from the nebular condensation trajectory. The Ir (and other refractory PGE) abundances in the Ni-rich metal clasts are higher than the expected values by up to ~30%.

Campbell et al. (2001a) also emphasized the importance of Pd in identifying condensation trends in metal; this is because Pd is not as refractory as Ir and the other PGEs and therefore Pd/Fe should not show high-temperature fractionations as large as those of Ir/Fe during condensation. Palladium can therefore be used to distinguish between a volatility-related process such as condensation and a redox process, which would produce Pd/Fe fractionations that are as large as those of Ir/Fe (Campbell et al., 2001a). Figure 4 shows that, similarly to Ir, the Pd-Ni trend is significantly higher than the calculated condensation trajectory. This is most evident at high Ni contents, where the fractionation of Pd/Fe from its chondritic value is highest; the data at near-chondritic abundances do little to resolve the chemical processes affecting this metal. The Pd, Ir, and other PGE data do not support the proposal of Newsom and Drake (1979) that Bencubbin metal (and, by analogy, that of Weatherford and Gujba) formed by condensation from the solar nebula.

The effect of varying pressure on the solar gas equilibrium condensation calculations is also shown in Figure 4. For both Ir and Pd, the condensation trajectory shifts to higher PGE abundances at a given Ni abundance as the nebular pressure increases. This shift is too small, however, to permit the PGE data in Bencubbin, Weatherford, and

Gujba metal to be explained by condensation from the solar nebula. Increasing the dust/gas ratio, as proposed by Petaev et al. (2001) to explain compositional trends in QUE 94411 zoned metal, has an effect very similar to increasing the total nebular pressure by the same factor, because the condensation of PGEs is not affected by the partial pressure of H₂. The increase in nebular pressures that is required to match the observed PGE-Ni trends in Bencubbin, Weatherford, and Gujba metal is so great ($P_{\text{H}_2} \sim 1$ kbar) that one would not consider such conditions to belong to the solar nebula.

The presence of troilite within the metal clasts of Bencubbin, Weatherford, and Gujba has been particularly difficult to explain, given the compositional trends observed in the metal (Newsom and Drake, 1979). Sulfur is a volatile element but sulfides are present in significant amounts (up to ~1 vol%) in the interiors of these volatile-depleted, refractory-enriched metal clasts. Rubin et al. (2001), based on petrographic study and neutron activation analysis of several clasts in Gujba, propose two models of formation of Gujba metal: 1) quenching of a high-temperature metal-sulfide assemblage, followed by heating and partial evaporative loss of volatiles; and 2) condensation at high temperatures, followed by crystallization of a S-rich melt around the metal. Both of these models suffer from the same problem as the nebular condensation model discussed above, if it is assumed that the evaporation (in model 1) or condensation (in model 2) occurred in a gas that was similar to the solar nebula in composition and pressure; namely, the siderophile element abundances do not follow the calculated trajectory for equilibrium condensation (or evaporation) (Figure 4).

4.3 Non-nebular Condensation of Metal Alloy

We have established that the formation of chemical signatures in Bencubbin, Weatherford, and Gujba metal was governed by the volatilities of the elements, and also that this volatility-controlled process was not nebular condensation or evaporation. In this section non-nebular settings for the origin of this metal are considered. For example,

Kallemeyn et al. (2001) suggested that these meteorite components may have condensed from impact ejecta, in the manner in which Wasson and Kallemeyn (1990) interpreted the petrography of ALH 85085. Although there are difficulties with an impact origin of Bencubbin, as discussed in a later section, we pursue this scenario here because of the failure of nebular condensation models to explain the observed siderophile element correlations. A plume produced by impact between two planetesimals may have produced a wide range of pressure and temperature conditions in which impact-generated vapor could have condensed. In principle this model can be tested against the measured trace element patterns in the same way that nebular condensation was examined above. It is only necessary to extend the condensation calculations to the relatively high density conditions of an impact-produced vapor.

The suite of solar gas calculations displayed in Figure 4 gives an indication of the effects of increasing gas density on the condensation paths. As the gas density increases, the Pd/Fe vs. Ni/Fe path shifts upward, and a smaller upward shift is also seen in the Ir/Fe path. In order for the calculated condensation paths to match the Bencubbin-Weatherford-Gujba metal data, the calculations suggest that a much greater increase in the partial pressures of the siderophile elements is needed.

As a simple model of an impact plume, we consider a gas in which the siderophile elements only have been uniformly enriched relative to a solar gas. This is a reasonable approach because, to a great extent, metal alloy condenses independently of the silicate portion of the gas. In constructing the high-metal condensation trajectories, thermodynamic data for the liquid phase of the elements were used, anticipating the elevation of the condensation temperatures (T_c) above the melting point of Fe-rich alloy (Hultgren et al., 1973ab); in other respects the calculations are like those in Campbell et al. (2001a), which follow a procedure outlined by Palme and Wlotzka (1976) and Fegley and Palme (1985). Figure 6 shows the effect, on a few representative elements, of enriching the gas in metals by a factor of 10^7 , i.e. siderophile element abundances were increased in this calculation by

seven orders of magnitude, relative to a solar gas at 10^{-4} bar. Raising the partial pressure of metal in the gas raises the condensation temperature (Grossman, 1972). However, the T_c of each element is affected differently, because the Gibbs free energies of the elements have different temperature dependences. Under the 10^7 x metal-rich conditions in Figure 6, metallic alloy condenses as a liquid at ~ 2500 K (50% condensation temperature), and the initial partial pressure of Fe is 0.06 bar. Note that Ir remains highly refractory under metal-rich conditions, although its T_c is now closer to that of Fe. The other refractory siderophiles (Ru, Rh, W, Re, Os, Pt) also remain highly refractory; all of them are $>99\%$ condensed at the 50% condensation point of Fe. Palladium becomes more refractory relative to Fe than it was under solar nebula conditions (Figure 6). Metal-enrichment of the gas also enhances condensation of Cu into the alloy; at the 50% condensation point of Fe, Cu is about 3% condensed in the metal-enriched gas but only $<0.2\%$ condensed in the 10^{-4} bar solar nebula.

Condensation trajectories, using a metal enrichment factor of 10^7 , have been added to Figure 4, and the agreement in these figures between the high-metal condensation paths and the data is very good. The Ir-Ni trend is well-described by the calculation; recall that, because the refractory siderophiles are unfractionated from Ir, Figure 4 is equally representative of Ru, Rh, Re, Os, or Pt vs. Ni. At the low-Ni end of the calculated trend, the data fall slightly below the calculation. This may reflect 1) a small degree of fractional condensation; 2) that Weatherford and Gujba, to which these points correspond, were processed under slightly different conditions than Bencubbin; or 3) an initial gas composition that differs slightly from chondritic relative siderophile abundances. If it were assumed that the initial gas had a lower Ir/Fe ratio, perhaps near $1.7 \mu\text{g/g}$ so that it lay at the base of the trend defined by the data, then the metal enrichment required to match the data would be even greater than the factor of 10^7 used here. No metal enrichment factor for the gas succeeds in matching the two outlying data from Weatherford (Figure 4). Regardless, the high-metal condensation model is a significant improvement over the 10^{-4}

bar nebular condensation calculation in describing the refractory siderophile element signatures in these meteorites. Likewise, Figure 4 shows that at high metal partial pressures, Pd is significantly more refractory than Fe, and the data are again better described by equilibrium with a metal-enriched gas than with the solar nebula.

The comparison between nebular and metal-enriched condensation is continued in Figure 7, in which the condensation of several moderately volatile siderophile elements is modelled and compared to the data from metal clasts in Bencubbin, Weatherford, and Gujba. These data exhibit greater scatter than the more refractory elements in Figure 4, possibly due to their much lower abundances (Figure 2). However, the calculated abundances of these elements is very sensitive to the initial gas conditions (note the log scale in Figure 6), and the data are therefore still very useful in discriminating between a nebular or non-nebular condensation origin. The Cu data are much better described by the metal-enriched gas curve than by the solar nebula curve, with the exception of a few outlier points. The Ga data also lie closer to the metal-rich curve; the systematic shift in the data to lower abundances than predicted may represent partitioning of Ga between metal and the coexisting silicate, or the presence of a Ga-bearing gas species. There is a much smaller difference between the two condensation paths for Au, and the data are consistent with either curve, within the scatter. The calculated nebular condensation path for Sb lies far below the observed values, but Sb is much less volatile at higher gas densities, and the metal enrichment of the gas improves the fit to the data by over two orders of magnitude (Figure 7). The agreement between the LA-ICP-MS data on moderately volatile siderophiles and the high-density gas condensation calculation provides powerful support to the notion that the Bencubbin metal clasts formed by condensation or evaporation in a gas in which the siderophile elements were highly enriched, by several orders of magnitude, relative to the partial pressures of these elements expected in the early solar nebula.

Neither the calculations nor the data require a particular physical setting in which the gas could have achieved such high partial pressures. However, it is known that impact processes played an important role in early solar system dynamics, and on this account the model of Kallemeyn et al. (2001), in which the bencubbinites formed in a cloud of impact ejecta, deserves consideration. Any alternative mechanism for generating a dense, metal-rich gas would, in our view, be equally useful for generating the metal compositions, but no such alternative has been advanced. We have focussed on the siderophile abundances, for which we have obtained detailed measurements. In the next section the possible behavior of nonmetallic components in an impact cloud is considered.

4.4 Nonmetallic Components and Oxidation State of an Impact Cloud

An impact between two planetesimals would involve more than metallic components. Bencubbin is highly enriched in metal relative to most chondrites, but it does contain ~40% by volume of silicate material. The large chondrules in bencubbinites are nearly all barred olivine or cryptocrystalline types (Weisberg et al., 1990; 2001). These textures, in contrast to the porphyritic textures common in other chondrites, indicate quenching of a completely molten silicate droplet. Therefore the silicate clasts in the Bencubbin and related meteorites likely formed at high temperatures, above the silicate liquidus. The liquidus temperature of a typical Bencubbin silicate clast (Weisberg et al., 1990) is estimated to be 1810 K (Herzberg, 1979). As described by Ebel and Grossman (2000), the condensation temperature of silicates increases as the (silicate) dust fraction is increased in the gas, and at dust enrichments of 100x or higher (relative to a 10^{-3} bar solar gas), the first silicate phase to condense is a liquid. Therefore the chondrule textures documented by Weisberg et al. (1990; 2001) are in general agreement with formation at high temperatures in a gas having highly enriched lithophile element abundances.

A more quantitative comparison between Bencubbin silicates and the expected condensation sequence from a silicate-enriched gas, such as an impact plume, must await

silicate liquid condensation calculations covering the appropriate range of gas compositions. The calculations of Ebel and Grossman (2000) only extend to 1000x dust enrichments; if the impact cloud is assumed to have a metal/silicate ratio similar to the Bencubbinites, then lithophile enrichments of 10^5 - 10^6 would be inferred. Furthermore, Ebel and Grossman (2000) used a CI chondrite composition (Anders and Grevesse, 1989) as their model for dust. This choice forms a gas that is rather oxidizing, and will produce FeO-rich silicates early in the condensation sequence; indeed, the generation of oxidized iron was a principal motivation for dust-enrichment in the condensation calculations (Wood and Hashimoto, 1993; Ebel and Grossman, 2000). Bencubbinite silicates are Fe-poor, with $\text{FeO} \leq 5$ wt% (Weisberg et al., 2001), and it is therefore unlikely that they could have formed by condensation from the CI-dust enriched gas assumed by Ebel and Grossman (2000).

The high metal proportion and low-FeO silicate composition found in Bencubbin suggest that, if this meteorite represents the product of an impact plume, the two likely compositions of the impacting bodies are 1) a metal-rich body and 2) a reduced-silicate (low-FeO) body. Alternative pairs of impacting bodies could also be considered, provided that the resultant impact cloud is rich in metal and not very oxidizing. The agreement between the data and calculations in Figures 4 and 7 requires that the metal body have a bulk composition that approximates chondritic relative abundances, although volatile depletion might be allowable prior to the impact event. The composition of the silicate body is less constrained in the impact model, aside from the requirement that it have low FeO contents and little free oxygen with which to oxidize Fe in the metal. Unlike the metal clasts, that have a range of compositions that can be usefully compared to the calculated condensation trajectories, the chondrules in Bencubbin have a narrow range of major- and minor-element compositions (Weisberg et al., 1990). Although the silicates evidently span a range of compositions that produced both BO and CC chondrule textures, it is uncertain

whether this range is large enough to permit a silicate condensation analysis analogous to the models of metal formation in Figures 4 and 7.

With the constraint that the impact plume not be so oxidizing that Fe enters the silicates in large proportions, it should be considered whether the correlation between Mo/Ir and W/Ir observed in Bencubbin, Weatherford, and Gujba metal (Figure 5) could be the outcome of f_{O_2} variations within a plume. These variations could in principle have caused W and Mo depletions in the metal in either of two ways: 1) formation of gaseous oxides, in effect increasing the volatility of Mo and W; or 2) partitioning of Mo and W into the coexisting liquid silicate. Any alternative to the impact plume model must allow for a similar type of variation to explain the correspondence between Mo/Ir and W/Ir. Both gaseous oxide formation and metal/silicate partitioning can explain depletions in Mo/Ir and W/Ir, but not enrichments of the sort indicated by the high W/Ir points, relative to CI chondrite values, in Figure 5. The implication of the data at higher W/Ir in Figure 5 is that the bulk W/Ir ratio of the gas was greater than the CI value of 0.19. This conclusion is consistent with the W/Ir value of 0.24 measured by INAA in metal separates of Bencubbin by Kallemeyn et al. (1978). Bulk Mo data on Bencubbin are not available.

There are difficulties in producing the Mo and W variations in bencubbinite metals by gaseous Mo- and W-oxide formation. The Mo/Ir-W/Ir paths during condensation of metal alloy from a 10^7 x metal-enriched gas from 2700 K to 2100 K, with varying oxidation states, are plotted in Figure 5. (Similar curves, shifted to different termination points, could result from higher W/Ir and/or Mo/Ir values in the gas.) Here, the oxygen fugacity in the gas is given as the difference in log units from the iron-wüstite buffer; the solar nebula has an f_{O_2} of $\Delta IW \approx -6$ (Ebel and Grossman, 2000). The data in Figure 5 suggest that, if the Mo and W compositions of the metal alloy were influenced by $MoO_{x(g)}$ and $WO_{x(g)}$, then the f_{O_2} may have reached $\Delta IW \approx +0.5$. Such a high f_{O_2} would be expected to oxidize Fe to a much greater extent than is observed in both the siderophile element signatures of the metal, and the FeO content of the bencubbinite silicates. Furthermore, $MoO_{x(g)}$ and $WO_{x(g)}$

formation is highly temperature dependent, and this would produce correlations between W/Ir (or Mo/Ir) and Ir that are not observed (Figure 3). Therefore the Mo/Ir-W/Ir data probably do not reflect the influence of gaseous Mo- and W-oxide formation.

High-temperature partitioning between the liquid metal and coexisting silicate droplets can be evaluated with the compositions of bencubbinite metal and silicate clasts. The f_{O_2} at which the metal and silicate equilibrated can be estimated from the Fe contents of the two phases, using $\Delta IW = 2 \log (X_{FeO,sil}/X_{Fe,met})$ and assuming ideal behavior in the liquids (Hillgren et al., 1994). The mean compositions of silicate and metal in Bencubbin (Weisberg et al., 2001) indicate an oxygen fugacity of $\Delta IW \approx -3.2$; at 2400 K this is 2×10^{-9} bar, using data tabulated by Chase (1998) for Fe and FeO liquids. Measurements on Mo, W, and other redox-sensitive elements in the bencubbinite silicates should help elucidate this issue.

Sulfur was not included in the condensation calculations, because the activity coefficient of S in Fe-rich liquid is highly sensitive, in a complicated manner, to temperature and composition (Sharma and Chang, 1979). However, Newsom and Drake (1979) suggested that the sulfur present in Bencubbin metal may have resulted from condensation, either due to enhanced solubility of S in a condensing liquid alloy at high gas pressures, or from condensation of FeS-rich liquid in a relatively H_2 -depleted environment, in which the lack of H_2S will make S more available to the condensing phases. Ebel and Grossman (2000) have calculated that sulfide condensation begins at 1380 K in a solar gas with 1000x dust enrichment at 10^{-3} bar. Ebel and Grossman (2000) further conclude that direct condensation of sulfide liquids is likely in dust-enriched gas at 10^{-3} bar.

4.5 Physical Setting of Bencubbinite-forming Impact

Many workers have previously argued that chondrules were formed by impacts between molten planetesimals (Zook, 1981; Chen et al., 1998; Lugmair and Shukolyukov, 2001). Grossman (1988) and Boss (1996) reviewed arguments in favor of and against an

impact origin for chondrules. The specific impact scenario proposed here should be distinguished from these previous hypotheses, which were generic explanations for the origins of chondrules, since the evidence it is based upon applies to metal from a specific meteorite type, the Bencubbin-Weatherford-Gujba association, and not even to metal in related CR or CH chondrites. Further, Campbell et al. (2000; 2001a) showed that the origin of metal in QUE 94411 and HH 237 was consistent with condensation from a gas of solar composition at 10^{-4} bar [10 Pa] total pressure, interpreted to be a nebular setting. The results shown here for metal from the Bencubbin-Weatherford-Gujba association indicate that a distinct origin of this metal is required.

Models for impact origins of chondrules by Zook (1981) and Chen et al. (1998) involved impact disruption of molten planetesimals, where the energy required to melt the chondrules was provided by the decay of ^{26}Al ($t_{1/2} = 700,000$ years). The present impact hypothesis requires impact energy to vaporize the precursor material to form the high pressure vapor cloud in which the Bencubbin-Weatherford-Gujba metal condensed or devolatilized. This is envisioned to have occurred during hypervelocity impact between two asteroids, a relatively rare phenomenon. Bottke et al. (1994) provided frequency distributions of asteroidal collisions that indicate that only a small percentage of such collisions occur at pre-encounter velocities of $>8\text{-}10 \text{ km s}^{-1}$, sufficient to provide the energy required to vaporize chondritic material. The escape velocities of asteroids are low, typically $18 < v_{\text{esc}} < 180 \text{ m s}^{-1}$ for bodies with diameters $30 < d < 300 \text{ km}$. This poses a complication, since self-gravity is required to collect the debris from the impact and prevent its dispersal. Molecular velocities, $(3kT/m)^{1/2} \approx 1400 \text{ m s}^{-1}$ for a vapor at $T \geq 2500 \text{ K}$, would exceed the escape velocity of asteroidal-sized bodies (*e.g.*, 600 m s^{-1} for Ceres). A model in which Bencubbin metal was evaporating into, rather than condensing from, an impact-produced cloud is more likely to overcome the problem of formation prior to dispersal of the gas. The nature and timescale of the process envisaged here is distinct from

those inferred from zoned metal grains in QUE 94411 (Campbell et al., 2001a; Petaev et al., 2001).

Chen et al. (1998) speculated that the interiors of molten planetesimals may have been hot enough to partially vaporize material, and proposed that following disruption “condensation from such hot jets could begin at elevated 10^3 - 10^4 dynes/cm² [10^{-3} - 10^{-2} bar] pressures”, but do not address the physical concerns raised here about reagglomeration. Such a physical setting would require less energetic collisions, since most of the energy for melting and vaporization comes from decay of ²⁶Al, and the impact energy is mainly used to disrupt the molten planetesimal. Since such impacts would be fairly common, one would expect Bencubbin-like metal to be abundant in chondrites, which is not observed. Indeed, Chen et al. (1998) proposed their model for PGE fractionations in ordinary chondrites, which is not supported by direct measurements on OC metal (Humayun and Campbell, 2001). It is concluded that either hypervelocity impacts ($4.6 > T > 0$ Ga), or impact disruption of molten planetesimals within the first 2-5 M.y. of solar system history, could provide plausible physical settings for the condensation or evaporation of metal droplets in a high-pressure vapor cloud.

4.6 Radiometric Tests of the Impact Hypothesis for Bencubbin-Weatherford-Gujba Metal

Hypervelocity impacts are rare and continue to occur long after dissipation of the nebular disk. Thus, the impact events recorded in the IIE irons occurred over the time span 0.7-4.56 Ga, based on ⁸⁷Rb-⁸⁷Sr, ¹⁴⁷Sm-¹⁴³Nd, and ⁴⁰K-⁴⁰Ar dating (Burnett and Wasserburg, 1967; Bogard et al., 1967; Sanz et al., 1970; Bogard et al., 2000; Snyder et al., 2001). A catastrophic impact may have disrupted the L chondrite parent body at about 500 M.y. (Bogard et al., 1995). Siderophile element chronometers can provide geochronological constraints on the timing of formation of Bencubbin-Weatherford-Gujba metal by dating the chemical fractionations observed here. The Re/Os ratio is chondritic in

all metal fractions and would be of little utility. However, the range in W/Ir ratios observed (Figure 3) indicates that the Hf-W chronometer (*e.g.*, Lee and Halliday, 2000) could be applicable. Likewise, the Pd/Ag ratio is greatly enhanced in Bencubbin metal (Pd/Ag \geq 6000), which would give radiogenic $^{107}\text{Ag}/^{109}\text{Ag}$ ratios if this had occurred in the first 40-50 M.y. of solar system history (*e.g.*, Chen and Wasserburg, 1990). Nebular settings for the formation of Bencubbin-Weatherford-Gujba metal should yield ages with $T \leq 5$ M.y. (Podosek and Cassen, 1994). Similarly, impacts between molten planetesimals (Chen et al., 1998; Lugmair and Shukolyukov, 2001) must occur prior to ^{26}Al decay, $T \leq 2-3$ M.y. Radiometric age determinations of the silicates could be useful, but are neither directly applicable to the time of formation of the metal clasts/chondrules, nor free from subsequent impact resetting by processes that compacted the Bencubbinite meteorites (Weisberg et al., 2001).

4.7 Relationship of Bencubbin, Weatherford, and Gujba to Other CB

Chondrites and to CH and CR Chondrites

Regardless of whether the impact plume model is correct, our results on Bencubbin, Weatherford, and Gujba (the CB_a subgroup) imply that the metal component of these three members of the CB chondrite group had a different history than the zoned metal in QUE 94411 and HH 237 (the CB_b subgroup). This is important because metal constitutes ~60 vol% of these meteorites. In contrast to the present results for Bencubbin metal, Campbell et al. (2000; 2001a) showed that the PGE distributions in zoned metal grains in the CB_b chondrites are compatible with an origin by condensation from the solar nebula. One possibility is that QUE 94411 and HH 237 could represent unaltered material that was impacted and vaporized to form Bencubbin, Weatherford, and Gujba (A. Krot, private communication). Creating the CB_a meteorites from the CB_b meteorites might require little more than evaporating the CB_b material into a hot, dense gas and recondensing it, followed by admixture of unvaporized dust to contribute the light element isotopic

anomalies (Prombo and Clayton, 1978; Sugiura et al., 2000) to the re-accreted body. In this scenario the CB_b subgroup may still represent very primitive chondritic material, that holds clues to early nebular processes (Campbell et al., 2001a; Krot et al., 2001; Petaev et al., 2001; Weisberg et al., 2001). However, this scenario would also require that the large metal aggregates in the CB_b chondrites formed by a different process than those in the CB_a chondrites; siderophile element measurements on metal aggregates in QUE 94411 and HH 237 would help resolve this issue.

The CR chondrites share many compositional and isotopic characteristics with the CB group, and may also be considered as possible precursors to Bencubbin, Weatherford, and Gujba. The CB chondrites lie near the CR trend on an oxygen isotope plot (Weisberg et al., 2001), although the CR $\delta^{15}\text{N}$ values cluster around 160 ‰, significantly lower than Bencubbin and Weatherford (Kallemeyn et al., 1994; Weisberg et al., 1995). The volatility trends in bulk siderophile and lithophile abundances in CH chondrites are very similar to those in CB chondrites, with strong volatile depletions and moderate enrichments in highly refractory elements, although the CB group is more volatile depleted (Kallemeyn et al., 1994; Weisberg et al., 1995; 2001). However, the metal content of CR chondrites, ~7 vol% (Kallemeyn et al., 1994; Weisberg et al., 1995), is much lower than that of CB chondrites, 40-70 vol% (Weisberg et al., 2001; Rubin et al., 2001). The CR chondrules are mostly FeO-poor (Fa₁-Fa₅), but there is a small FeO-rich tail in this distribution and a few olivines reach Fa₂₀ or greater (Kallemeyn et al., 1994; Weisberg et al., 1995). Significant hydrothermal alteration has affected most CR chondrites, as evidenced by a highly oxidized matrix, with significant magnetite, and phyllosilicate-rich chondrule mesostases (Weisberg et al., 1993; Kallemeyn et al., 1994; Weisberg et al., 1995). This high oxygen content may eliminate CR meteorites as possible precursors to Bencubbin.

Compositionally, the CH (ALH 85085-like) chondrites are intermediate between the CR and CB groups: they have ~20 vol% metal and low matrix abundance (5 vol%); they are more volatile-depleted than the CR average but less so than Bencubbin; and they have

low-FeO silicates ($\sim\text{Fa}_2$) and show little evidence of metamorphism or aqueous alteration (Scott, 1988; Weisberg et al., 1995). The CH chondrites also lie on the CR oxygen isotope line, and ALH 85085 has a $\delta^{15}\text{N}$ of 858, close to that of Bencubbin (Weisberg et al., 1995). If CH-type chondrites are imagined to be impact precursors to Bencubbin, then a mechanism would be required to enhance the metal content, such as impact with a metal-rich body or perhaps size/density sorting during settling from the impact cloud.

5. CONCLUSIONS

The siderophile element abundances reported here are essential to constraining the origin of the host metal in Bencubbin and the related meteorites Weatherford and Gujba. The siderophile element abundances in this metal reflect the volatility of each element, and were not established by igneous/magmatic processes, nor by loss of Fe during oxidation of the metal. Comparison of the data to equilibrium condensation calculations reveals that the metal could not have formed by condensation (or evaporation) from the canonical solar nebula ($P_{\text{H}_2} \sim 10^{-3} - 10^{-6}$ bar), but that it could have formed by condensation (or evaporation) of liquid alloy from a highly metal-enriched gas, in which the siderophile elements were uniformly enriched by a factor of 10^7 relative to a 10^{-4} bar solar gas. On this basis it is suggested that Bencubbin, Weatherford, and Gujba may have formed in a vapor cloud induced by an impact involving a metal-rich body (Kallemeyn et al., 2001). The data do not require that the metal-rich gas formed by an impact; however, this is the only mechanism that has yet been suggested for generating such a gas. This model requires high energies to vaporize the shock-heated material; this could have been provided either by a rare, high-velocity impact, or by impact disruption of radioactively heated, molten planetesimals.

The host metals in Bencubbin, Weatherford, and Gujba have a shared history that is different from that of most metal in the other two CB chondrites, QUE 94411 and HH 237, which contain zoned metal grains that bear evidence of gas-solid condensation from a gas

similar to the solar nebula in composition and pressure (Campbell et al., 2001a).

Bencubbin, Weatherford, and Gujba are less primitive, in the sense that they appear to have a non-nebular origin. Based on their bulk compositional similarities, QUE 94411 and HH 237 are possible precursor materials from which Bencubbin, Weatherford, and Gujba may have formed. Other candidate precursors include CH-type chondrites; these have lower metal contents but may represent a silicate portion of Bencubbin.

Acknowledgments—We are grateful for the loan of specimens of Bencubbin from A. M. Davis, Weatherford from the American Museum of Natural History, and Gujba from A. E. Rubin. Discussions with D. Ebel, L. Grossman, A. Krot, and A. Meibom were beneficial, and reviews by A. Meibom, A. Krot, and T. McCoy were also very helpful. This work was supported by NASA NAG 5-9800 to M. H. and NAG 5-4745 to M. K. W.

REFERENCES

- Anders E. and Grevesse N. (1989) Abundances of the elements: Meteoritic and solar. *Geochim. Cosmochim. Acta* **53**, 197-214.
- Bogard D., Burnett D., Eberhardt P. and Wasserburg G. J. (1967) ^{40}Ar - ^{40}K ages of silicate inclusions in iron meteorites. *Earth Planet. Sci. Lett.* **3**, 275-283.
- Bogard D. D., Garrison D. H., Norman M., Scott E. R. D. and Keil K. (1995) ^{39}Ar - ^{40}Ar age and petrology of Chico: Large-scale impact melting on the L chondrite parent body. *Geochim. Cosmochim. Acta* **59**, 1383-1399.
- Bogard D. D., Garrison D. H. and McCoy T. J. (2000) Chronology and petrology of silicates from IIE iron meteorites: Evidence of a complex parent body evolution. *Geochim. Cosmochim. Acta* **64**, 2133-2154.
- Boss A. P. (1996) A concise guide to chondrule formation models. In *Chondrules and the Protoplanetary Disk* (eds. R. H. Hewins, R. H. Jones and E. R. D. Scott). Cambridge Univ. Press, Cambridge. pp. 257-263.
- Bottke, Jr., W. F., Nolan M. C., Greenberg R. and Kolvoord R. A. (1994) Velocity distributions among colliding asteroids. *Icarus* **107**, 255-268.
- Buchwald V. F. (1975) *Handbook of Iron Meteorites*. Univ. California Press, Berkeley.
- Burnett D. and Wasserburg G. J. (1967) Evidence for the formation of an iron meteorite at 3.8×10^9 years. *Earth Planet. Sci. Lett.* **2**, 137-147.
- Campbell A. J. and Humayun M. (1999a) Trace element microanalysis in iron meteorites by laser ablation ICPMS. *Anal. Chem.* **71**, 939-946.
- Campbell A. J. and Humayun M. (1999b) Microanalysis of platinum group elements in iron meteorites using laser ablation ICP-MS. *Lunar Planet. Sci. XXX*. Lunar Planet. Inst., Houston. #1974 (abstr.).
- Campbell A. J. and Humayun M. (2000) Trace siderophile element distributions in Bencubbin metal. *Meteorit. Planet. Sci.* **35**, A38.

- Campbell A. J., Humayun M. and Weisberg M. K. (2000) Siderophile element distributions in zoned metal grains in Hammadah al Hamra 237. *Meteorit. Planet. Sci.* **35**, A38-A39.
- Campbell A. J., Humayun M., Meibom A., Krot A. N. and Keil K. (2001a) Origin of zoned metal grains in the QUE94411 chondrite. *Geochim. Cosmochim. Acta* **65**, 163-180.
- Campbell A. J., Humayun M. and Weisberg M. K. (2001b) Siderophile element concentrations in bencubbinite metals. *Lunar Planet. Sci. XXXII*. Lunar Planet. Inst., Houston. #1842 (abstr.).
- Chase, Jr., M. W. (1998) *NIST-JANAF Thermochemical Tables*, 4th ed. *J. Phys. Chem. Ref. Data* Monograph No. 9. American Institute of Physics, Woodbury, New York.
- Chen J. H. and Wasserburg G. J. (1990) The isotopic composition of Ag in meteorites and the presence of ^{107}Pd in protoplanets. *Geochim. Cosmochim. Acta* **54**, 1729-1743.
- Chen J. H., Papanastassiou D. A. and Wasserburg G. J. (1998) Re-Os systematics in chondrites and the fractionation of the platinum group elements in the early solar system. *Geochim. Cosmochim. Acta* **62**, 3379-3392.
- Ebel D. and Grossman L. (2000) Condensation in dust-enriched systems. *Geochim. Cosmochim. Acta* **64**, 339-366.
- Fegley, Jr., B. and Palme H. (1985) Evidence for oxidizing conditions in the solar nebula from Mo and W depletions in refractory inclusions in carbonaceous chondrites. *Earth Planet. Sci. Lett.* **72**, 311-326.
- Grossman J. N. (1988) Formation of chondrules. In *Meteorites and the Early Solar System* (eds. J. F. Kerridge and M. S. Matthews). Univ. Arizona Press, Tucson. pp. 680-696.
- Grossman L. (1972) Condensation in the primitive solar nebula. *Geochim. Cosmochim. Acta* **36**, 597-619.

- Grossman L. and Olsen E. (1974) Origin of the high-temperature fraction of C2 chondrites. *Geochim. Cosmochim. Acta* **38**, 173-187.
- Herzberg C. T. (1979) The solubility of olivine in basaltic liquids: an ionic model. *Geochim. Cosmochim. Acta* **43**, 1241-1251.
- Hillgren V. J., Drake M. J. and Rubie D. C. (1994) High-pressure and high-temperature experiments on core-mantle segregation in the accreting Earth. *Science* **264**, 1442-1445.
- Hultgren R., Desai P. D., Hawkins D. T., Gleiser M. and Kelley K. K. (1973a) *Selected Values of the Thermodynamic Properties of Binary Alloys*. American Society for Metals, Metals Park, Ohio.
- Hultgren R., Desai P. D., Hawkins D. T., Gleiser M., Kelley K. K. and Wagman D. D. (1973b) *Selected Values of the Thermodynamic Properties of the Elements*. American Society for Metals, Metals Park, Ohio.
- Humayun M. and Campbell A. J. (2001) The duration of ordinary chondrite metamorphism inferred from tungsten microdistribution in OC metal. *Lunar Planet. Sci. XXXII*. Lunar Planet. Inst., Houston. #2102 (abstr.).
- Jones J. H. and Malvin D. J. (1990) A nonmetal interaction model for the segregation of trace metals during solidification of Fe-Ni-S, Fe-Ni-P, and Fe-Ni-S-P alloys. *Metall. Trans. B* **21B**, 697-706.
- Kallemeyn G. W., Boynton W. V., Willis J. and Wasson J. T. (1978) Formation of the Bencubbin polymict meteoritic breccia. *Geochim. Cosmochim. Acta* **42**, 507-515.
- Kallemeyn G. W., Rubin A. E. and Wasson J. T. (1994) The compositional classification of chondrites: VI. The CR carbonaceous chondrite group. *Geochim. Cosmochim. Acta* **58**, 2873-2888.
- Kallemeyn G. W., Rubin A. E. and Wasson J. T. (2001) Compositional studies of Bencubbin dark silicate host and an OC clast: Relationships to other meteorites and

- implications for their origin. *Lunar Planet. Sci. XXXII*. Lunar Planet. Inst., Houston. #2070 (abstr.).
- Krot A. N., Meibom A., Russell S. S., Alexander C. M. O'D., Jeffries T. E. and Keil K. (2001) A new astrophysical setting for chondrule formation. *Science* **291**, 1776-1779.
- Lee D.-C. and Halliday A. N. (2000) Hf-W internal isochrons for ordinary chondrites and the initial $^{182}\text{Hf}/^{180}\text{Hf}$ of the solar system. *Chem. Geol.* **169**, 35-43.
- Lee M. S., Rubin A. E. and Wasson J. T. (1992) Origin of metallic Fe-Ni in Renazzo and related chondrites. *Geochim. Cosmochim. Acta* **56**, 2521-2533.
- Lugmair G. W. and Galer S. J. G. (1992) Age and isotopic relationships among the angrites Lewis Cliff-86010 and Angra-Dos-Reis. *Geochim. Cosmochim. Acta* **56**, 1673-1694.
- Lugmair G. W. and Shukolyukov A. (2001) Early solar system events and time scales. Submitted to *Meteorit. Planet. Sci.*
- Meibom A., Petaev M. I., Krot A. N., Wood J. A. and Keil K. (1999) Primitive FeNi metal grains in CH carbonaceous chondrites formed by condensation from a gas of solar composition. *J. Geophys. Res.* **104**, 22053-22059.
- Meibom A., Desch S. J., Krot A. N., Cuzzi J. N., Petaev M. I., Wilson L. and Keil K. (2000) Large scale thermal events in the solar nebula recorded in Fe, Ni metal condensates in primitive meteorites. *Science* **288**, 839-841.
- Newsom H. E. and Drake M. J. (1979) The origin of metal clasts in the Bencubbin meteorite breccia. *Geochim. Cosmochim. Acta* **43**, 689-707.
- Palme H. and Wlotzka F. (1976) A metal particle from a Ca,Al-rich inclusion from the meteorite Allende, and the condensation of refractory siderophile elements. *Earth Planet. Sci. Lett.* **33**, 45-60.

- Petaev M. I., Meibom A., Krot A. N., Wood J. A. and Keil K. (2001) The condensation origin of zoned metal grains in Queen Alexandra Range 94411: Implications for the formation of the Bencubbin-like chondrites. *Meteorit. Planet. Sci.* **36**, 93-106.
- Podosek F. A. and Cassen P. (1994) Theoretical, observational, and isotopic estimates of the lifetime of the solar nebula. *Meteoritics* **29**, 6-25.
- Prombo C. A. and Clayton R. N. (1985) A striking nitrogen isotope anomaly in the Bencubbin and Weatherford meteorites. *Science* **230**, 935-937.
- Ramdohr P. (1973) *The Opaque Minerals in Stony Meteorites*. Elsevier, Amsterdam.
- Rubin A. E., Kallemeyn G. W., Wasson J. T., Clayton R. N., Mayeda T. K., Grady M. M. and Verchovsky A. B. (2001) Gujba: A new Bencubbin-like meteorite fall from Nigeria. *Lunar Planet. Sci. XXXII*. Lunar Planet. Inst., Houston. #1779 (abstr.).
- Sanz H. G., Burnett D. S. and Wasserburg G. J. (1970) A precise $^{87}\text{Rb}/^{87}\text{Sr}$ age and initial $^{87}\text{Sr}/^{86}\text{Sr}$ for the Colomera iron meteorite. *Geochim. Cosmochim. Acta* **34**, 1227-1239.
- Scott E. R. D. (1988) A new kind of primitive chondrite, Allan Hills 85085. *Earth Plan. Sci. Lett.* **91**, 1-18.
- Sharma R. C. and Chang Y. A. (1979) Thermodynamics and phase relationships of transition metal-sulfur systems: Part III. Thermodynamic properties of the Fe-S liquid phase and the calculation of the Fe-S phase diagram. *Metall. Trans. B* **10B**, 103-108.
- Snyder G. A., Lee D.-C., Ruzicka A. M., Prinz M., Taylor L. A. and Halliday A. N. (2001) Hf-W, Sm-Nd, and Rb-Sr isotopic evidence of late impact fractionation and mixing of silicates on iron meteorite parent bodies. *Earth Plan. Sci. Lett.* **186**, 311-324.
- Sugiura N., Zashu S., Weisberg M. K. and Prinz M. (2000) A nitrogen isotope study of Bencubbinites. *Meteorit. Planet. Sci.* **35**, 987-996.

- Sylvester P. J., Ward B. J., Grossman L. and Hutcheon I. D. (1990) Chemical compositions of siderophile element-rich opaque assemblages in an Allende inclusion. *Geochim. Cosmochim. Acta* **54**, 3491-3508.
- Wai C. M. and Wasson J. T. (1977) Nebular condensation of moderately volatile elements and their abundances in ordinary chondrites. *Earth Planet. Sci. Lett.* **36**, 1-13.
- Wänke H., Dreibus G., Jagoutz E., Palme H. and Rammensee W. (1981) Chemistry of the Earth and the significance of primary and secondary objects for the formation of planets and meteorite parent bodies. *Lunar Planet. Sci.* **XII**, 1139-1141.
- Wasson J. T. and Kallemeyn G. W. (1990) Allan Hills 85085: A subchondritic meteorite of mixed nebular and regolithic heritage. *Earth Planet. Sci. Lett.* **101**, 148-161.
- Wänke H., Dreibus G., Jagoutz E., Palme H. and Rammensee W. (1981) Chemistry of the Earth and the significance of primary and secondary objects for the formation of planets and meteorite parent bodies. *Lunar Planet. Sci.* **XII**, 1139-1141.
- Wasson J. T., Ouyang X., Wang J. and Jerde E. (1989) Chemical classification of iron meteorites: XI. Multi-element studies of 38 new irons and the high abundance of ungrouped irons from Antarctica. *Geochim. Cosmochim. Acta* **53**, 735-744.
- Weisberg M. K., Prinz M. and Nehru C. E. (1990) The Bencubbin chondrite breccia and its relationship to CR chondrites and the ALH85085 chondrite. *Meteoritics* **25**, 269-279.
- Weisberg M. K., Prinz M., Clayton R. N. and Mayeda T. K. (1993) The CR (Renazzo-type) carbonaceous chondrite group and its implications. *Geochim. Cosmochim. Acta* **57**, 1567-1586.
- Weisberg M. K., Prinz M., Clayton R. N., Mayeda T. K., Grady M. M. and Pillinger C. T. (1995) The CR chondrite clan. *Proc. NIPR Symp. Antarct. Meteorites* **8**, 11-32.
- Weisberg M. K., Prinz M., Clayton R. N., Mayeda T. K., Sugiura N. and Zashu S. (1998) The bencubbinite (B) group of the CR clan. *Meteorit. Planet. Sci.* **33**, A166.

- Weisberg M. K., Prinz M., Clayton R. N., Mayeda T. K., Sugiura N., Zashu S. and Ebihara M. (1999) QUE94411 and the origin of bencubbinites. *Lunar Planet. Sci.* XXX. Lunar Planet. Inst., Houston. #1416 (abstr.).
- Weisberg M. K., Prinz M., Humayun M. and Campbell A. J. (2000) Origin of metal in the CB (bencubbinite) chondrites. *Lunar Planet. Sci.* XXXI. Lunar Planet. Inst., Houston. #1466 (abstr.).
- Weisberg M. K., Prinz M., Clayton R. N., Mayeda T. K., Sugiura N., Zashu S. and Ebihara M. (2001) A new metal-rich chondrite group. *Meteorit. Planet. Sci.* **36**, 401-418.
- Wood J. A. and Hashimoto A. (1993) Mineral equilibrium in fractionated nebular systems. *Geochim. Cosmochim. Acta* **57**, 2377-2388.
- Zanda B., Bourot-Denise M., Perron C. and Hewins R. H. (1994) Origin and metamorphic redistribution of silicon, chromium, and phosphorus in the metal of chondrites. *Science* **265**, 1846-1849.
- Zook H. A. (1981) On a new model for the generation of chondrules. *Lunar Planet. Sci.* **XII**, 1242-1244.

TABLES

Table 1. Laser ablation ICP-MS standards. Underlined entries indicate values used in calibration. Italicized entries denote detection limits. Data in ppm unless indicated otherwise. Errors are 2σ . Literature values from: Buchwald, 1975; Wasson et al., 1989; Sylvester et al., 1990; Campbell and Humayun, 1999b. Reference values for SRM 1263a and SRM 1158 are values certified by NIST.

	Hoba		Filomena		SRM1263		SRM1158	
	measured	lit.	measured	lit.	measured	ref.	measured	ref.
P	551 ± 22	700	2004 ± 1014	3000	290 ± 46	<u>290</u>	87 ± 11	40
S	62 ± 8		89 ± 5		54 ± 4	<u>57</u>	57 ± 5	<u>50</u>
Fe wt%	82.79 ± 0	82.79	93.6 ± 0	93.8	94.4 ± 0	94.4	64.7 ± 0	63.8
Co	7801 ± 144	<u>7800</u>	4470 ± 59	4540	445 ± 3	480	68 ± 1	80
Ni wt%	16.4 ± 0.2	<u>16.4</u>	5.8 ± 0.3	5.65	0.307 ± 0.002	0.320	34.3 ± 0.5	36.03
Cu	6 ± 3		150 ± 6	134	973 ± 14	<u>980</u>	401 ± 20	<u>390</u>
Ga	0.22 ± 0.02	0.19	59 ± 3	<u>58.8</u>	13.1 ± 0.3		5.1 ± 0.3	
Ge	<i>0.4</i>	0.035	176 ± 12	<u>177</u>	23.4 ± 0.4		8.9 ± 0.7	
As	0.6 ± 0.2		4.7 ± 0.5	<u>4.73</u>	99.5 ± 1.1	<u>100</u>	31 ± 7	
Mo	24.8 ± 1.1		8.1 ± 1.5		292 ± 12	<u>300</u>	105 ± 6	<u>100</u>
Ru	28.6 ± 0.8	<u>28.6</u>	17.7 ± 0.8	17.6	0.029 ± 0.026		1.80 ± 0.05	
Rh	4.9 ± 0.2	<u>4.86</u>	3.1 ± 0.3		0.107 ± 0.010		0.03 ± 0.02	
Pd	6.7 ± 0.3	<u>6.65</u>	1.95 ± 0.12		0.09 ± 0.05		0.08 ± 0.05	
Sn	0.6 ± 0.4		0.38 ± 0.13		1040 ± 35	<u>1040</u>	28 ± 8	
Sb	0.19 ± 0.05		0.5 ± 0.5		20 ± 1	<u>20</u>	7 ± 2	
W	2.99 ± 0.08		2.5 ± 0.2	<u>2.562</u>	464 ± 32	<u>460</u>	14.0 ± 0.3	
Re	3.15 ± 0.08	<u>3.15</u>	0.24 ± 0.04	0.234	0.010 ± 0.004		0.017 ± 0.008	
Os	42.5 ± 0.7	<u>42.5</u>	1.12 ± 0.07	1.06	0.006 ± 0.004		0.006 ± 0.003	
Ir	29.1 ± 0.4	<u>29.1</u>	3.77 ± 0.16	3.37	0.010 ± 0.004		0.005 ± 0.001	
Pt	28.6 ± 0.5	<u>28.6</u>	23.9 ± 0.3	20.7	0.025 ± 0.017		<i>0.005</i>	
Au	0.088 ± 0.015	<u>0.084</u>	0.59 ± 0.07	0.612	4.7 ± 0.4	<u>5</u>	<i>0.003</i>	

Table 2. Laser ablation ICP-MS data from metal in the bencubbinites Bencubbin, Weatherford, and Gujba. Italicized entries denote detection limits. Errors are 2σ .

wt%:		P	S	Cr	Fe	Co	Ni	
Bencubbin	clast A	0.34 ± 0.04	0.5 ± 0.3	0.20 ± 0.05	92.2 ± 0.4	0.30 ± 0.01	6.5 ± 0.3	
	clast B	0.44 ± 0.04	0.5 ± 0.3	0.18 ± 0.05	91.5 ± 0.4	0.327 ± 0.009	7.1 ± 0.2	
	clast C	0.32 ± 0.02	0.2	0.34 ± 0.02	92.6 ± 5.1	0.31 ± 0.02	6.4 ± 0.4	
	clast D	0.26 ± 0.02	0.31 ± 0.09	0.27 ± 0.01	92.2 ± 0.1	0.311 ± 0.007	6.64 ± 0.03	
	clast 5	0.43 ± 0.05	0.9 ± 0.8	0.18 ± 0.01	91.9 ± 0.4	0.29 ± 0.03	6.3 ± 0.4	
	clast 6	0.34 ± 0.03	1.1 ± 0.3	0.17 ± 0.01	91.9 ± 5.1	0.30 ± 0.02	6.2 ± 0.3	
	clast 20	0.38 ± 0.03	0.3 ± 0.2	0.17 ± 0.01	91.8 ± 5.1	0.32 ± 0.02	6.9 ± 0.4	
	clast 21	0.37 ± 0.02	0.8 ± 0.2	0.16 ± 0.01	92.2 ± 5.1	0.28 ± 0.02	6.1 ± 0.3	
	clast 22	0.41 ± 0.03	0.9 ± 0.2	0.16 ± 0.01	92.1 ± 5.1	0.31 ± 0.02	6.1 ± 0.3	
Gujba	clast 23	0.33 ± 0.02	1.3 ± 0.2	0.23 ± 0.01	92.1 ± 5.1	0.28 ± 0.02	5.8 ± 0.3	
	clast A	0.21 ± 0.01	0.174 ± 0.006		94.1 ± 0.1	0.292 ± 0.005	5.79 ± 0.08	
	clast B	0.22 ± 0.01	0.047 ± 0.003		93.6 ± 5.1	0.32 ± 0.02	6.3 ± 0.3	
Weatherford	clast C	0.17 ± 0.01	0.091 ± 0.008		93.6 ± 0.1	0.307 ± 0.003	6.21 ± 0.05	
	clast A	0.25 ± 0.01	0.21 ± 0.07		93.6 ± 0.4	0.308 ± 0.003	6.2 ± 0.1	
	clast N	0.25 ± 0.04	0.18 ± 0.07		94.0 ± 0.1	0.28 ± 0.01	5.8 ± 0.2	
	clast M	0.23 ± 0.01	0.24 ± 0.07		94.0 ± 0.1	0.279 ± 0.002	5.8 ± 0.1	
	clast S	0.25 ± 0.04	0.22 ± 0.03		94.3 ± 0.2	0.272 ± 0.003	5.6 ± 0.3	

ppm:		Cu	Ga	Ge	As	Mo	Ru	Rh	Pd
Bencubbin	clast A	100 ± 70	1.80 ± 0.09	0.68 ± 0.08	4.1 ± 0.1	7.6 ± 0.6	4.9 ± 0.6	1.2 ± 0.1	3.3 ± 0.3
	clast B	90 ± 20	2.71 ± 0.07	0.76 ± 0.09	5.4 ± 0.2	7.3 ± 0.4	6.2 ± 0.7	1.6 ± 0.2	3.9 ± 0.4
	clast C	6.5 ± 0.8	0.43 ± 0.01	0.11 ± 0.03	2.1 ± 0.1	5.9 ± 0.6	4.2 ± 0.5	1.1 ± 0.1	3.5 ± 0.5
	clast D	6.2 ± 0.5	0.53 ± 0.02	0.12 ± 0.05	2.5 ± 0.2	6.2 ± 0.1	5.2 ± 0.2	1.3 ± 0.1	3.1 ± 0.1
	clast 5	109 ± 5	2.2 ± 0.1	1.2 ± 0.4	5.3 ± 0.6	5.5 ± 0.3	4.5 ± 0.5	1.0 ± 0.2	3.5 ± 0.4
	clast 6	90 ± 6	1.2 ± 0.8	0.98		3.6 ± 0.6	3.1 ± 0.6	0.8 ± 0.1	3.4 ± 0.5
	clast 20	78 ± 5	2.1 ± 0.7	0.9 ± 0.8		7.4 ± 0.8	6.4 ± 0.7	1.4 ± 0.2	3.9 ± 0.5
	clast 21	74 ± 5	2.1 ± 0.3	0.5 ± 0.1	5.8 ± 0.8	4.5 ± 0.6	3.0 ± 0.5	0.8 ± 0.1	2.7 ± 0.4
	clast 22	76 ± 5	1.6 ± 0.7	1.2 ± 0.8		4.4 ± 0.6	3.7 ± 0.6	0.8 ± 0.1	2.6 ± 0.4
Gujba	clast 23	140 ± 8	2.3 ± 0.1	1.0 ± 0.4	6.0 ± 0.8	5.2 ± 0.6	4.0 ± 0.5	0.9 ± 0.1	2.9 ± 0.4
	clast A	129 ± 4	3.1 ± 0.2	1.31 ± 0.02	4.3 ± 0.1	3.7 ± 0.1	3.3 ± 0.1	0.75 ± 0.01	2.7 ± 0.1
	clast B	134 ± 8	2.5 ± 0.4	0.91	4.4 ± 1.5	5.1 ± 0.8	4.0 ± 0.6	0.9 ± 0.2	3.0 ± 0.7
Weatherford	clast C	12.4 ± 0.4	0.61 ± 0.01	0.17 ± 0.03	2.2 ± 0.2	6.1 ± 0.2	4.5 ± 0.2	0.97 ± 0.04	2.9 ± 0.2
	clast A	150 ± 10	3.5 ± 0.3	1.47 ± 0.04	4.8 ± 0.1	9.9 ± 0.2	6.9 ± 0.3	1.64 ± 0.05	3.4 ± 0.3
	clast N	250 ± 80	2.1 ± 0.2	0.66 ± 0.01	4.6 ± 0.3	9.4 ± 0.2	6.6 ± 0.2	1.65 ± 0.03	3.3 ± 0.2
	clast M	59 ± 1	1.3 ± 0.1	0.41 ± 0.06	3.8 ± 0.1	4.4 ± 0.1	3.4 ± 0.1	0.79 ± 0.01	3.1 ± 0.1
	clast S	330 ± 310	2.1 ± 0.3	0.5 ± 0.2	5.4 ± 0.3	3.5 ± 0.4	2.9 ± 0.3	0.60 ± 0.09	2.56 ± 0.03

Table 2 (continued).

ppm:	Sn	Sb	W	Re	Os	Ir	Pt	Au	
Bencubbin	clast A		0.09 ± 0.04	1.4 ± 0.5	0.32 ± 0.06	4.1 ± 0.2	3.5 ± 0.2	6.4 ± 0.3	0.63 ± 0.08
	clast B		0.12 ± 0.02	0.8 ± 0.1	0.36 ± 0.05	4.7 ± 0.4	4.4 ± 0.3	8.4 ± 0.7	0.80 ± 0.06
	clast C		0.10 ± 0.01	0.8 ± 0.1	0.23 ± 0.05	3.6 ± 0.3	3.0 ± 0.2	5.6 ± 0.5	0.29 ± 0.07
	clast D		0.11 ± 0.02	0.4 ± 0.1	0.345 ± 0.002	4.0 ± 0.2	3.6 ± 0.1	6.6 ± 0.1	0.34 ± 0.06
	clast 5		0.56 ± 0.15	0.8 ± 0.1	0.27 ± 0.02	3.0 ± 0.1	3.1 ± 0.2	5.6 ± 0.2	0.85 ± 0.04
	clast 6			0.3 ± 0.1	0.27 ± 0.07	3.3 ± 0.3	2.8 ± 0.2	5.2 ± 0.5	0.70 ± 0.14
	clast 20			0.6 ± 0.1	0.28 ± 0.07	4.4 ± 0.3	4.0 ± 0.3	7.5 ± 0.6	0.77 ± 0.13
	clast 21		0.37 ± 0.06	0.3 ± 0.1	0.33 ± 0.07	3.0 ± 0.3	2.7 ± 0.2	5.0 ± 0.4	0.64 ± 0.12
	clast 22			0.3 ± 0.1	0.32 ± 0.07	3.0 ± 0.3	2.7 ± 0.2	4.9 ± 0.5	0.67 ± 0.12
	clast 23		0.34 ± 0.05	0.8 ± 0.1	0.21 ± 0.05	2.9 ± 0.2	2.6 ± 0.2	4.6 ± 0.4	0.67 ± 0.10
Gujba	clast A	0.16 ± 0.03	0.047 ± 0.002	0.32 ± 0.02	0.21 ± 0.02	2.34 ± 0.06	2.1 ± 0.1	3.6 ± 0.1	0.42 ± 0.01
	clast B	0.51	0.118	0.54 ± 0.12	0.50 ± 0.09	3.2 ± 0.3	3.2 ± 0.3	5.3 ± 0.5	0.46 ± 0.10
	clast C	0.13 ± 0.02	0.025 ± 0.004	0.78 ± 0.03	0.27 ± 0.01	3.03 ± 0.04	3.0 ± 0.1	5.1 ± 0.2	0.24 ± 0.01
Weatherford	clast A	0.16 ± 0.03	0.06 ± 0.02	1.23 ± 0.02	0.42 ± 0.01	4.9 ± 0.2	4.9 ± 0.3	8.5 ± 0.4	0.48 ± 0.02
	clast N	0.16 ± 0.05	0.06 ± 0.01	1.30 ± 0.16	0.32 ± 0.03	3.7 ± 0.1	4.2 ± 0.3	7.6 ± 0.7	0.41 ± 0.03
	clast M	0.08 ± 0.01	0.05 ± 0.01	0.53 ± 0.01	0.22 ± 0.01	2.46 ± 0.05	2.3 ± 0.1	3.9 ± 0.0	0.34 ± 0.02
	clast S	0.22	0.13 ± 0.07	0.36 ± 0.03	0.17 ± 0.06	1.97 ± 0.02	1.7 ± 0.1	2.8 ± 0.2	0.53 ± 0.04

FIGURE CAPTIONS

Figure 1. Backscattered electron image of a) Bencubbin and b) Weatherford. In the clast on the left of a), metal grains that are sulfide-free and that contain rounded sulfide blebs are sintered together with arcuate sulfide occurring at the grain margins. The clast on the right of a) contains few sulfides. The Weatherford clast in b) has a similar texture to the large Bencubbin clast on the left in a). Scale bars are a) 2 mm, b) 0.5 mm.

Figure 2. Siderophile element abundances in Bencubbin, Weatherford, and Gujba metal clasts, normalized to Fe and CI abundances (Anders and Grevesse, 1989). Data below detection limits are not shown. Open circles are bulk INAA data from Bencubbin (Kallemeyn et al., 1978).

Figure 3. Abundance ratios of Mo, Ru, Rh, Pd, W, Re, Os, Pt, and Au to Ir in Bencubbin (circles), Gujba (squares), and Weatherford (triangles) metal clasts. The dashed lines are chondritic values (Anders and Grevesse, 1989). The refractory siderophiles strongly correlate with one another in nearly chondritic proportions, although Mo and W show more scatter than the others. The non-refractory siderophiles Pd and Au are fractionated from Ir at high Ir concentrations.

Figure 4. Ir/Fe vs. Ni/Fe (top) and Pd/Fe vs. Ni/Fe (bottom) for metal clasts in Bencubbin (circles), Gujba (squares), and Weatherford (triangles). The chondritic abundances (Anders and Grevesse, 1989) are represented by the solid square. The addition/removal of Fe during redox processing is represented by the thin solid line. Calculated equilibrium condensation trajectories, at nebular pressures of 10^{-6} (bottom), 10^{-4} (middle), and 10^{-2} (top) bar are indicated by heavy dotted lines. The condensation trajectory of a gas that is metal-enriched by a factor of 10^7 , relative to the nebular conditions, is shown as a heavy solid line. Data from within a single zoned metal grain in QUE 94411 (Campbell et al.,

2001a) are shown as solid diamonds; 2σ errors on these points are $\sim 20\%$. Note that the QUE 94411 data and the Bencubbin data follow different trends in Pd/Fe vs. Ni/Fe.

Figure 5. Mo/Ir vs. W/Ir for metal clasts in Bencubbin (circles), Gujba (squares), and Weatherford (triangles). Scaling these elements against Ir allows the effect of oxidation to be observed independently of the refractory behavior of Mo and W. The chondritic abundances are represented by the solid square. Solid curves represent condensation paths in a metal-enriched ($10^7\times$) gas, with various oxidation fugacities indicated by their difference in log units from the iron-wüstite buffer.

Figure 6. Condensation curves for Fe, Cu, Pd, and Ir under nebular and metal-rich conditions. Gray curves, at lower temperatures, represent condensation of solid metal alloy from a solar gas at 10^{-4} bar total pressure. Black curves, at higher temperatures, represent condensation of liquid metal alloy from a gas that is uniformly enriched in the siderophile elements by a factor of 10^7 relative to the solar gas. Note that Pd is significantly more refractory than Fe in the metal-rich gas, in contrast to its behavior in solar gas, while Ir is highly refractory relative to Fe in both cases.

Figure 7. Volatile element abundances in Bencubbin, Weatherford, and Gujba metal clasts, compared to the calculated condensation paths for a solar nebula at 10^{-4} bar (dashed curves) and a gas that is metal-enriched by a factor of 10^7 relative to the nebular conditions (solid curves). Upper figure: Cu (solid circles / black curves), Ga (open circles / gray curves); lower figure: Sb (solid circles / black curves), Au (open circles / gray curves). Chondritic compositions are indicated by solid squares.

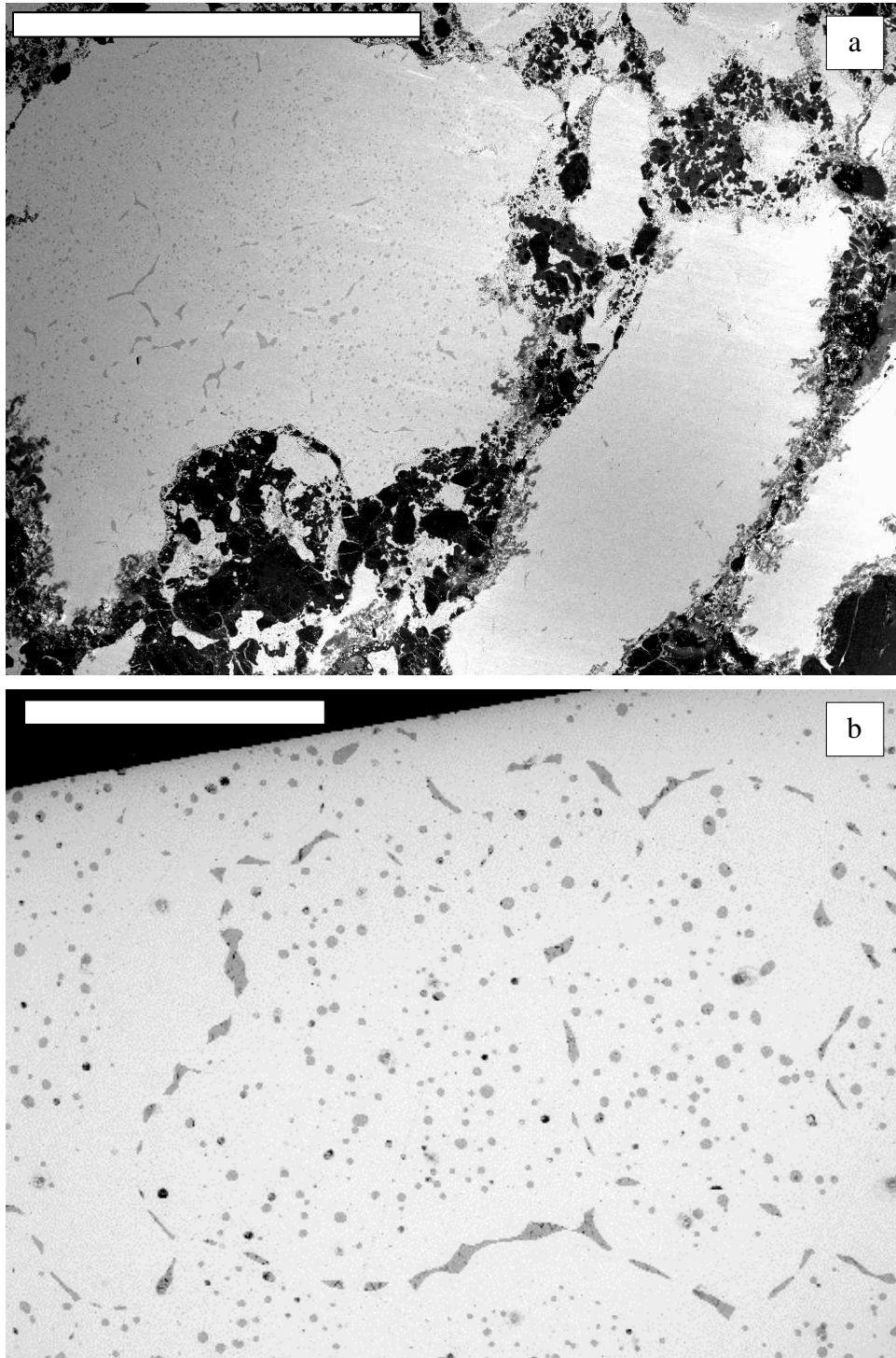


Figure 1

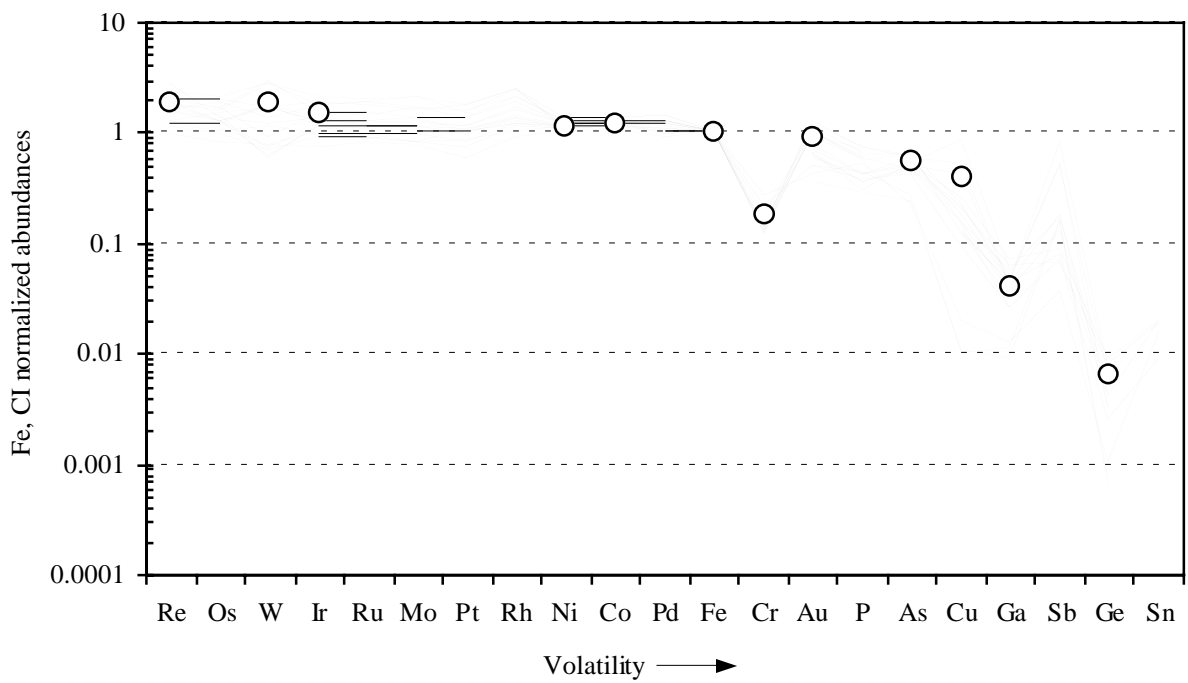


Figure 2

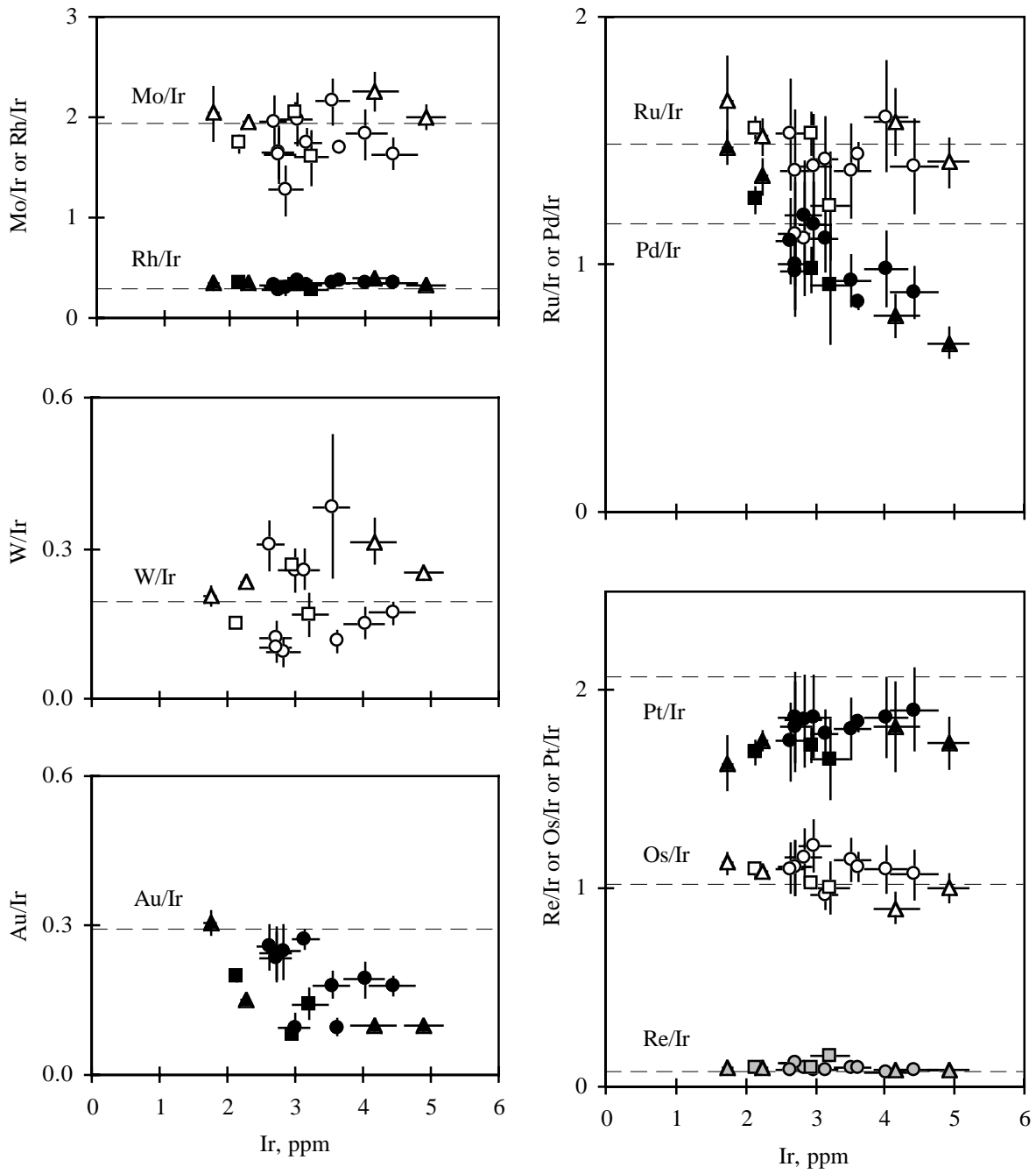


Figure 3

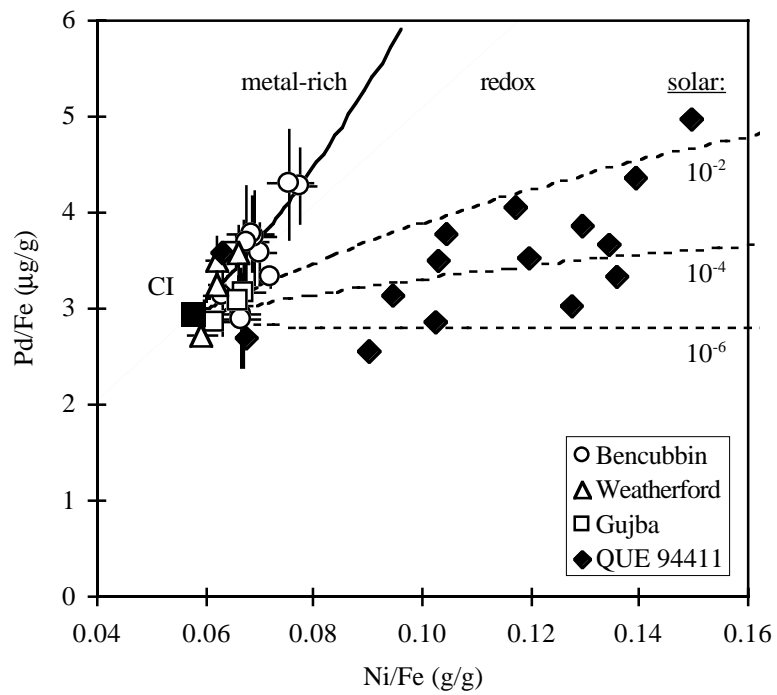
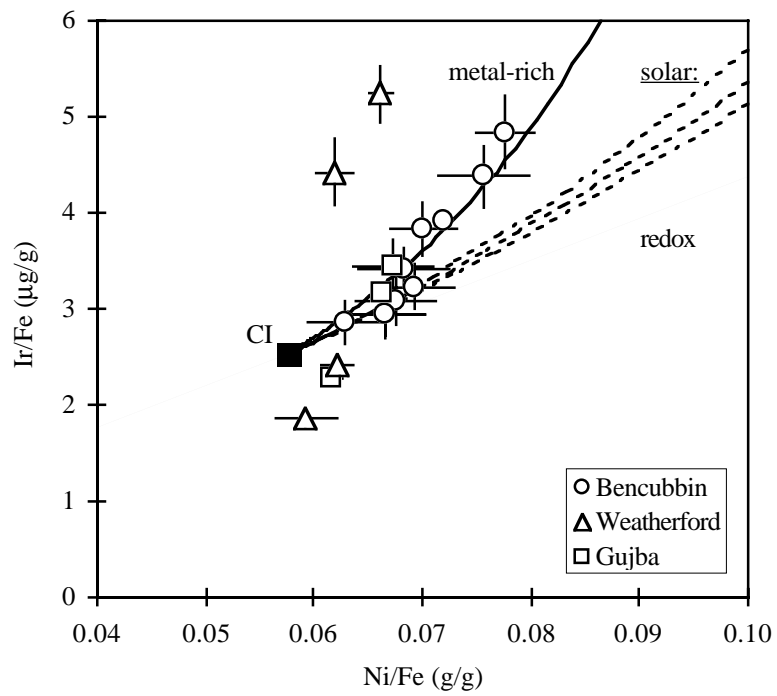


Figure 4

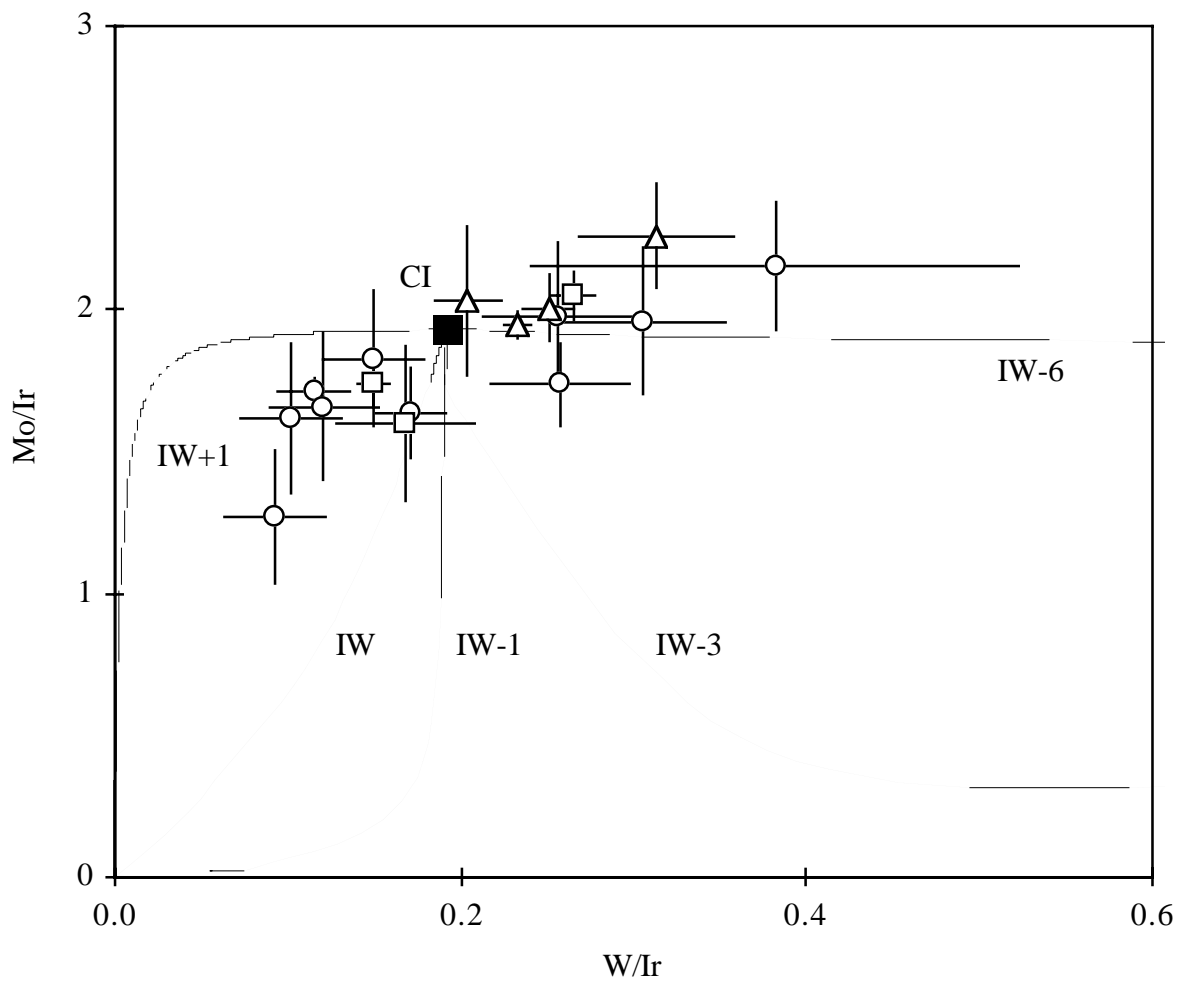


Figure 5

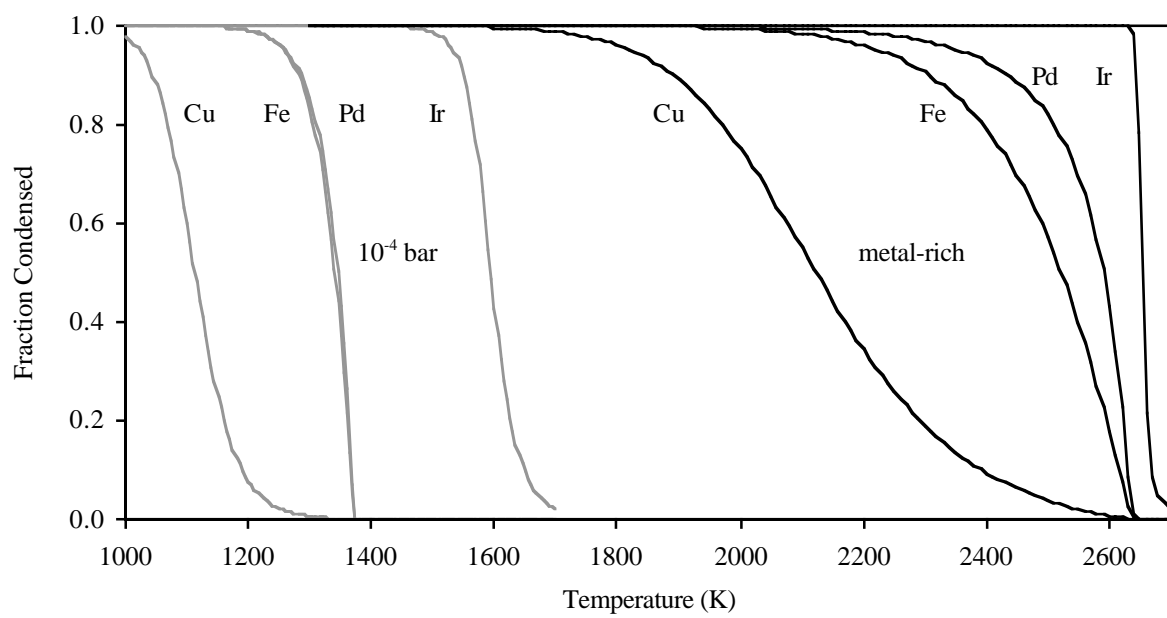


Figure 6

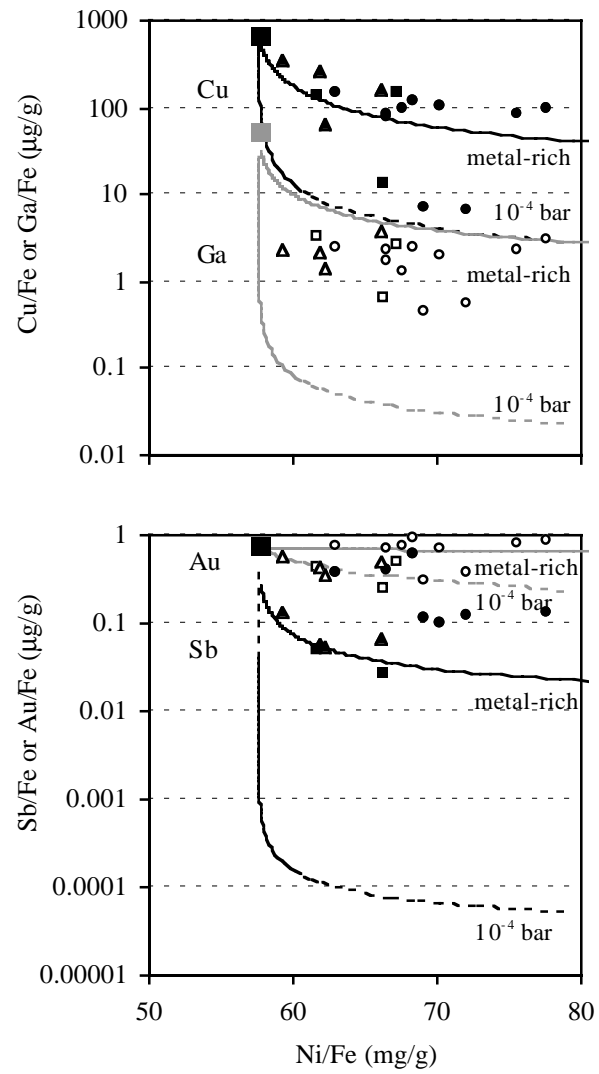


Figure 7